# 4. Shock Metamorphism ❖❖❖

Shock-metamorphic products have become one of the diagnostic tools of impact cratering studies. They have become the main criteria used to identify structures of impact origin. They have also been used to map the distribution of shock-pressures throughout an impact target. The diverse styles of shock metamorphism include fracturing of crystals, formation of microcrystalline planes of glass through crystals, conversion of crystals to high-pressure polymorphs, conversion of crystals to glass without loss of textural integrity, conversion of crystals to melts that may or may not mix with melts from other crystals.

Shock-metamorphism of target lithologies at the crater was first described by Barringer (1905, 1910) and Tilghman (1905), who recognized three different products. The first altered material they identified is rock flour, which they concluded was pulverized Coconino sandstone. Barringer observed that rock flour was composed of fragmented quartz crystals that were far smaller in size than the unaffected quartz grains in normal Coconino sandstone. Most of the pulverized silica he examined passed through a 200 mesh screen, indicating grain sizes <74 µm (0.074 mm), which is far smaller than the 0.2 mm average detrital grain size in normal Coconino (Table 2.1). Fairchild (1907) and Merrill (1908) also report a dramatic comminution of Coconino, although only 50% of Fairchild's sample of rock flour passed through a 100 mesh screen, indicating grain sizes <149 µm. Heterogeneity of the rock flour is evident in areas where sandstone clasts survive within the rock flour. The rock flour is pervasive and a major component of the debris at the crater. Barringer estimated that 15 to 20% of the ejecta is composed of rock flour.

He also noted that surviving rock fragments of Coconino in the debris deposits are altered, describing a Variety A sandstone (which is lightly to moderately shocked sandstone with a greater density than unaffected Coconino) and a Variety B sandstone (which was melted, is vesicular, and will float on water). Variety A sandstone is distributed within the rock flour. According to Tilghman (as recorded by Merrill, 1908), it constitutes ~2% of the sandstone debris and ranges in size from fractions of an inch to blocks 10 to 12 ft in diameter. One of the boreholes apparently penetrated a 50 ft block 500 ft below the crater floor. Barringer (1910) noted that Variety A shock-metamorphosed sandstone is far more abundant than the pumiceous Variety B sandstone, but also suggests that Variety B material may have decomposed over time and be partly responsible for rock flour. As far as I know, a quantitative microscopic study of the rock flour and the relative proportions of different types of silica components in it has not been done to evaluate this suggestion.

Based on a microscopic examination of crater lithologies in thin-section, Merrill (1908, after Diller) began to augment Barringer's shock-classification of the sandstone. The initial phase of shock crushed the sandstone, reduced porosity, and created fractures in quartz grains where they collided. In a second phase of shock-metamorphism, the interlocking of the quartz is so complete that the sandstone resembles a holocrystalline rock. The quartz also often has undulatory extinction. He suggests the quartz was altered under intense pressure and deformed "in an almost putty-like or plastic condition." Rocks shocked to this state also have interstitial pockets of a nearly isotropic, fibrous, and scaly material that has the composition of opal (silica with water). In the third stage of shock-metamorphism, the rocks become increasingly vesicular or pumiceous glass with relict grains of unaltered quartz. Merrill wrote that the damage was limited to samples of the Coconino. He could not find any deformation in cores of the underlying Supai sandstone, recovered beneath the breccia lens, that were available at the time. He wrote that "in no instance did they show any signs whatever of the shattering, fusion, or metamorphism so characteristic of the overlying white sandstone [Coconino]."

The next contribution to the study of shock metamorphism at the crater was provided by Rogers (1928) in his Presidential Address to The Mineralogical Society of America. He recognized that some of the silica glass (lechatelierite) in Variety B shock-metamorphosed sandstone has the same texture as quartz in unaffected sandstone, writing that "Lechateliérite (silica glass) ... retains the granular texture from which it was derived" and that the lechateliérite grains are "paramorphs ... after quartz." This characteristic shock-metamorphic material is generically called thetamorphic or diaplectic glass today (*e.g.*, Chao, 1967; Stöffler, 1972).

In some of the dominantly sheared, yet granular Coconino, it was eventually realized that some pockets of suspected glass or devitrified glass (the nearly isotropic pockets of Merrill) were instead coesite, a high-pressure polymorph of silica. Indeed, the first natural occurrence of coesite was found at Meteor Crater (Chao *et al.*, 1960) and has become another important criterion for identifying an impact crater. Soon thereafter, another high-pressure polymorph of silica, stishovite, was also found at the crater (Chao *et al.*, 1962). Chao and his colleagues reported that both phases occur in Variety A sandstones and survive as a minor constituent in the melted Variety B sandstone.

Kieffer (1971, 1976) continued the detailed examination of shocked Coconino in an effort to expand upon the shock-metamorphic sequence that occurs in the rocks and, where possible, interpret them in the context of the mechanics of the rock's interaction with a passing shock wave. She divided shocked samples into the five classes recognized today:

Class 1. Initially, the porosity of the rocks was reduced, largely by grain rotation, but no fracturing of quartz grains occurs (Class 1a). At slightly higher shock conditions, the grains began to fracture and may have small amounts of plastic deformation (Class 1b). The fractures appear to have been produced by concussion when neighboring grains collide, because the fractures often radiate from the point of contact between grains. Class 1a rocks have remnant porosity, but Class 1b rocks do not. Class 1 rocks do not contain any higher pressure silica polymorphs.

Class 2. The porosity of the Coconino was completely consumed as grains deformed plastically, forming a puzzle-like fabric. Symplektic pockets occur between grains where pores once existed. Coesite formed in the symplektic regions. These rocks will be 80 to 95% quartz, 2 to 5% coesite, 3 to 10% glass, and have no detectable stishovite.

Class 3. Like class 2 rocks, plastic flow of quartz collapsed the pore space. Coesite is abundant in cryptocrystalline pockets and stishovite begins to appear in opaque regions that surround the coesite-bearing cryptocrystalline pockets. Estimates for the amount of coesite range from 18 to 32% in these rocks, in addition to 0 to 20% glass and traces of stishovite.

Class 4. Vesicular glass formed adjacent to coesite-rimmed quartz grains. Only 15 to 45% of the original quartz survives. These samples have abundant coesite (10 to 30%) and glass (20 to 75%). They do not have any detectable stishovite using optical microscope techniques.

Class 5. This is an extreme version of class 4, where the glass and vesicles dominate the rock and only a few quartz relicts survive. These samples are 80 to 100% glass, with 0 to 15% quartz and 0 to 5% coesite. Most samples that can still be recovered at the surface are only 1 to 5 centimeters thick, although I have seen blocks of this glass that are ~15 cm thick.

Unlike quartz-bearing crystalline target rocks (*e.g.*, granites and gneisses), the shocked Coconino sandstone has very few planar shock features (either fractures or closer-space lamellae). Typically less than 5% of the grains in Class 2 or 3 rocks have planar features. This reflects one of the important differences between impact cratering events in crystalline targets and sedimentary targets. In the latter, a

greater fraction of the impact energy is consumed closing pore space, so that there are fewer solid state transformations and higher post-shock temperatures than similar impacts into crystalline targets.

Increasing shock pressures also destroyed fluid inclusions that occurred in the Coconino sandstone (Elwood Madden *et al.*, 2006). Two-phase inclusions begin to disappear under Class 1 conditions and are completely gone in Class 3 samples. The number of inclusions in Class 1 and 2 samples, however, remains the same, as the two-phase inclusions are transformed into single-phase inclusions. The total number of inclusions in Class 3 and 4 rocks are lower, indicating that fluid inclusions are destroyed by the plastic deformation and phase changes that occur under those shock conditions. Very few one-phase inclusions survive in Class 4 and 5 samples. Thus, crystal components in the sandstone are dehydrated by shock-metamorphism.

In contrast to these extensive studies of Coconino sandstone, very little is known about the effects of solid phase shock transformation in the Moenkopi and Kaibab Formations. The Moenkopi shales and siltstones are so fine-grained that optical microscope identification of any shock transformation that may have occurred is difficult. The Moenkopi also represents the free surface of the impact site, which would have reduced the volume that saw peak shock presssures in excess of 5 GPa (Fig. 3.7). Shock-metamorphism in the carbonate fraction of the Kaibab is a challenge to study, because it is difficult to discriminate shock-induced deformation from other types of geologic deformation in that type of material. Carbonate is too easily deformed to be used routinely for shock-metamorphic studies. Nonetheless, samples from Barringer Crater probably offer one of the best opportunities to document the progression of deformation that occurs in dolomite; it may be worth further study. It might also be interesting to determine how the quartz fraction within the Kaibab has been affected by shock (both where it is embedded within carbonate and where it occurs in isolated beds of sandstone).

At higher shock levels, target rocks are melted. Melts from individual phases are mixed, producing "normal melts" or "mixed melt," that are distributed in deposits of mixed debris inside the crater and deposits of alluvium on the outermost flanks of the crater. Some of these mixed melts also entrain fractions of the impacting asteroid.

Impact-generated melts at the crater were first described by Nininger (1954, 1956). The melts range in morphology from melt splashes that encompass clasts of target rock (Fig. 4.1) to a variety of isolated aerodynamic forms, although most specimens are irregularly shaped with pitted (and often vesicular) surfaces. The largest clasts found with melt splashes were 5 to 6 cm in length and composed of Coconino sandstone. Molten particles collided with each other in flight, because some melt fragments have compound droplet morphologies. Melt particle colors have many different colors, although they are usually shades of gray, brown, and red-stained brown in bulk form. Yellow and bright red colors are often evident in thin-section. The melt particles (or, at least those that are easily recoverable) range in size from a millimeter to a few centimeters. The volume of total melt produced is still debated and is hard to evaluate now because of the extensive effects of erosion (which stripped the fall-out unit around the crater) and previous collections of melt. Nininger (1956) reported that most melts were within 1,500 ft (~460 m) of the crater rim and that none were found beyond 1 ½ mi (2.4 km) from the crater rim.

Before describing the Barringer Crater melts further, it might be useful to make some general comments about impact melts. One of the oft-spoken attributes of impact melts is their homogeneity. In large complex craters with substantial impact melt sheets, the melt is often a homogenized mixture of the complex target lithologies that were melted. Only subtle compositional variations have been reported. There must always be an exception to prove the rule and that exception is Sudbury. In that case the melt sheet is heterogeneous, because of post-impact igneous differentiation.

In contrast, melts that are ejected from a crater are often incompletely mixed. For example, in the

case of Chicxulub, which involved a diverse target assemblage of carbonates and silicates, a range of Ca-rich to Ca-poor melt droplets were deposited in moderately distal ejecta deposits.

In simple impact craters, like Barringer, there is not sufficient molten material to form a coherent melt sheet. Even in the larger (4 km diameter) Brent simple crater in Canada, only sufficient melt to form pods within a breccia lens was generated. In Barringer Crater, there is no detectable melt pods within the breccia lens. Nor are there any significant melt pools on the crater walls and in the ejecta blanket. There was either an insufficient volume of melt produced by the impact event and/or it was too finely disseminated (possibly because of a relative high volatile content in the target rocks; Kieffer and Simonds, 1980) to produce those types of deposits. Melts were locally produced within the transient cavity and not well mixed. In addition, a highly disparate proportion of projectile material was added to the melts. A relatively large range of melt compositions is the result.

A preliminary petrographic study of Barringer Crater melts was generated during the Apollo era by Greenwood and Morrison (1969), who reported that Fe,Ni-metal was entrained in the melt and that the silicate fraction of the melt precipitated olivine, actinolite, and magnetite. Much more detail, however, was recently revealed by Hörz *et al.* (2002) and See *et al.* (2002), who thoroughly studied the chemical compositions of target strata and 80 melt particles generated from them. They confirmed that the melts contain immiscible Fe-Ni metal alloys and sulfides from the projectile, although they also noted that the metal and sulfide often have chemically fractionated compositions. Nickel is enhanced in the metal and sulfide. The abundance of FeO from target lithologies is on the order of 2 wt%, yet FeO contents of the silicate portions of the melts are often 25 to 30 wt%. The enhanced FeO is attributed to oxidation of meteoritic iron component from the projectile, which is consistent with the Ni/Fe fractionation in the metal and sulfide. In principal, it is possible that some of the FeO in the silicate impact melts came from silicate inclusions within the type IAB iron asteroid. Inclusions in type IAB meteorites are generally about 70% mafic silicates (olivine and pyroxene), 10% sodic plagioclase, 10% metal, 10% sulfide. However, in the specific case of the Canyon Diablo meteoritic fragments, silicates are usually associated with troilite-graphite nodules, which represent about 8.5% of the meteorites (Buchwald, 1975). Silicates in Canyon Diablo specimens are much less common than in other type IAB meteorites, so they are not likely to be a significant source of FeO. Hörz *et al.* (2002) found that the projectile component is greater in melts that have a significant Kaibab component and less in those that have a larger Moenkopi component. This is consistent with models in which the projectile passes through the thin Moenkopi cover and penetrates the underlying Kaibab.

A significant fraction of the projectile-derived FeO was incorporated into olivine and pyroxene that precipitated from the impact melt. Olivine and pyroxene compositions vary considerably between melt particles (and within some melt particles). These two phases are not in equilibrium with each other, nor with the surviving metal alloys entrained in the melts. The crystallization of olivine and pyroxene in a sedimentary province or, in this case, in melts generated from sedimentary siltstone, dolomite, and sandstone, is unusual. It appears that $CO_2$ in the target carbonate was driven off, forming refractory (Ca, Mg, and Fe-rich) residues that mixed with Si and meteoritic components. Most of the melts are highly vesicular, which is further testament to the thorough loss of target volatiles. A preliminary study of impact melts by another group (Kargel *et al*., 1996) also reported 100% decarbonation of melted Kaibab.

Many of the melt particles have regions that produce low analytical totals (typically 70 to 90 wt%), implying a volatile component (*e.g.*, $H_2O$, OH, CO, or $CO_2$) exists within them. Hörz *et al.* (2002) and See *et al.* (2002) heated several representative samples to drive off any gases and analyze them. Only water vapor was detected, which is probably the result of post-impact oxidation and hydration rather than an inherent property of the melts. No CO or $CO_2$ was detected, indicating that component of the target carbonates was thoroughly excised during the formation of the large collection of melts studied.

Although almost all melts studied suggest strong degassing, small amounts of $CO_2$-charged impact melt appear to have also been produced. Thin-layers and veneers of melts with carbonate-like compositions have been recovered (Fig. 4.2 and 4.3). Although a direct detection of $CO_2$ has not yet been reported, analytical totals are consistent with a $CO_2$ rather than $H_2O$ component. The presumed $CO_2$-charged melts are in direct contact with refractory olivine and pyroxene-bearing melts that are highly vesiculated and that were obviously degassed. Although the silicate-dominated melts were thoroughly degassed, the splashes of $CO_2$-charged melts imply there were small batches of melts that did not degas. Presumably, they were heated to temperatures needed for melting, but not hot enough to degas or were quenched before degassing could occur.

Interestingly, a quench zone of carbonate crystals along the boundary of the carbonate-dominated melt in Fig. 4.2 suggests an un-degassed molten sample collided with a previously degassed melt that had already solidified. This illustrates the complexity and speed with which material is affected by the impact event and mixed.

Observations at Barringer Crater, in addition to those at craters with larger melt volumes, imply a two-step mixing process for crater melts: (1) mixing of projectile material with local (stratigraphically-limited) target melts and (2) mixing of those melts along the crater wall to produced a homogeneous melt composition. In the case of Barringer Crater, step (1) occurred, but (2) did not occur or only partially occurred, because there is tremendous heterogeneity among silicate melt compositions, in addition to the sharp contrast between silicate-dominated and carbonate-dominated melts. Either there was not sufficient melt volume along the crater wall to facilitate homogenizing melt mixing or the material was ejected before that mixing could occur. The high volatile content of the target lithologies (11 wt% for Moenkopi and 27 wt% for Kaibab; See *et al.*, 2002) may have triggered an early and/or particularly violent disruption of melt volumes and expansion out of the crater.

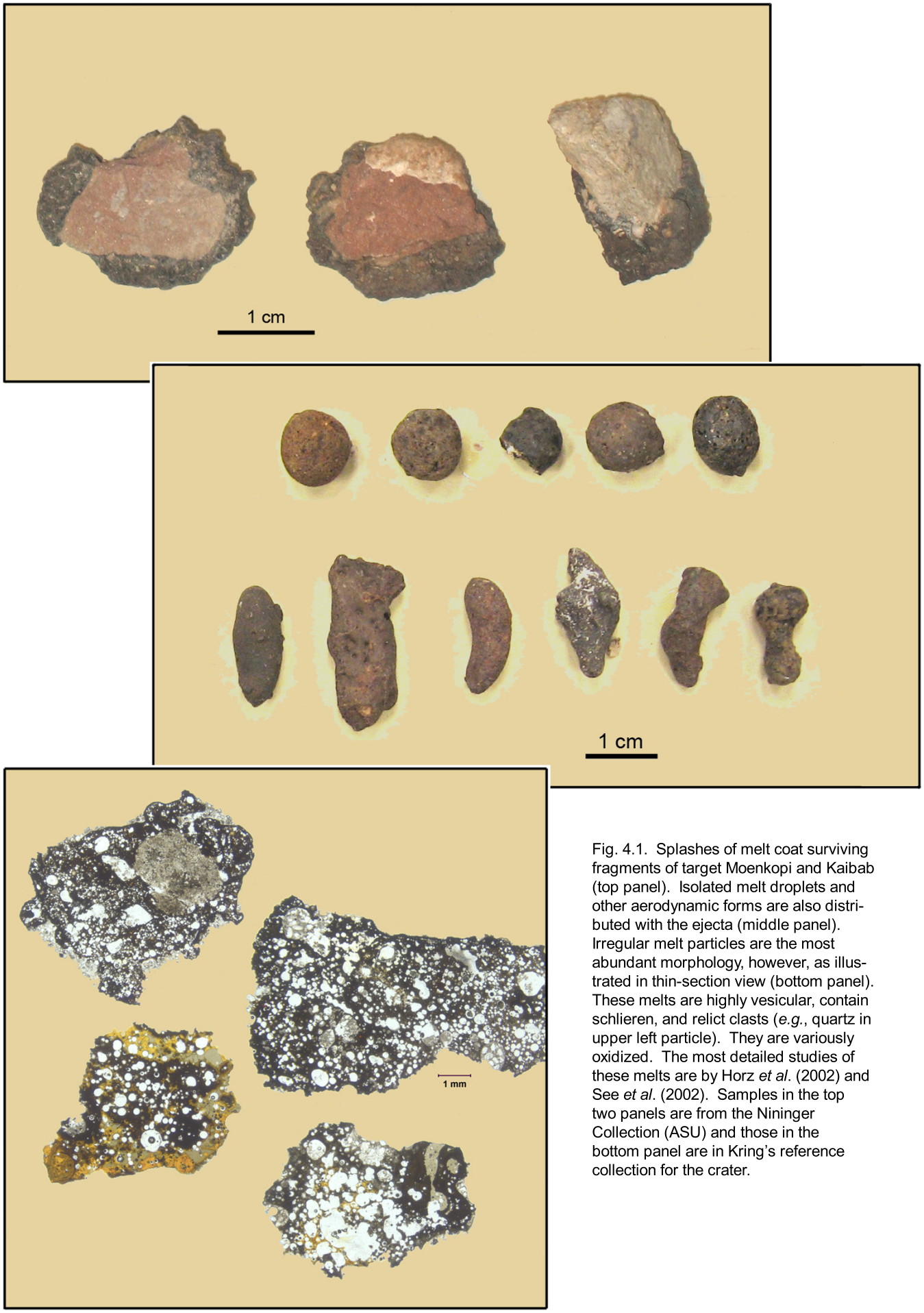


Fig. 4.1. Splashes of melt coat surviving fragments of target Moenkopi and Kaibab (top panel). Isolated melt droplets and other aerodynamic forms are also distributed with the ejecta (middle panel). Irregular melt particles are the most abundant morphology, however, as illustrated in thin-section view (bottom panel). These melts are highly vesicular, contain schlieren, and relict clasts (*e.g.*, quartz in upper left particle). They are variously oxidized. The most detailed studies of these melts are by Horz *et al*. (2002) and See *et al*. (2002). Samples in the top two panels are from the Nininger Collection (ASU) and those in the bottom panel are in Kring's reference collection for the crater.

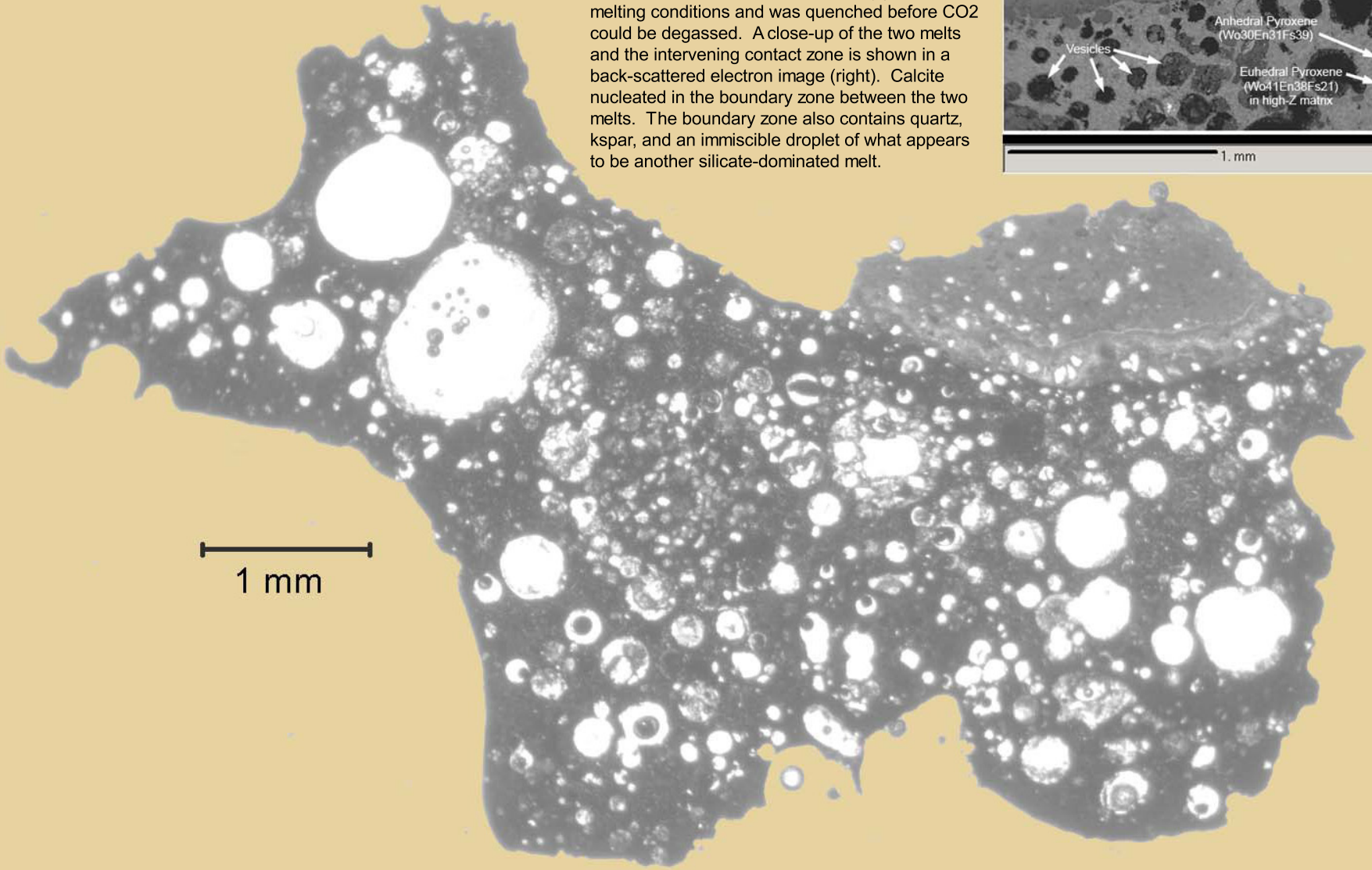


Fig. 4.2. Compound impact melt particle, shown in thin-section (below). The bulk of this melt particle is composed of a highly vesicular mafic silicate melt with relict quartz grains. Pyroxene crystallized from the melt while it was cooling from its initial superheated state. The melt is similar to those described by Horz *et al*. (2002), which formed from impact melted, and thoroughly degassed Kaibab, with variable contributions from the projectile (mostly Fe, Ni), Moenkopi (Si) and Coconino (Si). This silicate-dominated melt collided with a carbonate-dominated melt. The carbonate-dominated melt apparently just reached melting conditions and was quenched before CO2 could be degassed. A close-up of the two melts and the intervening contact zone is shown in a back-scattered electron image (right). Calcite nucleated in the boundary zone between the two melts. The boundary zone also contains quartz, kspar, and an immiscible droplet of what appears to be another silicate-dominated melt.

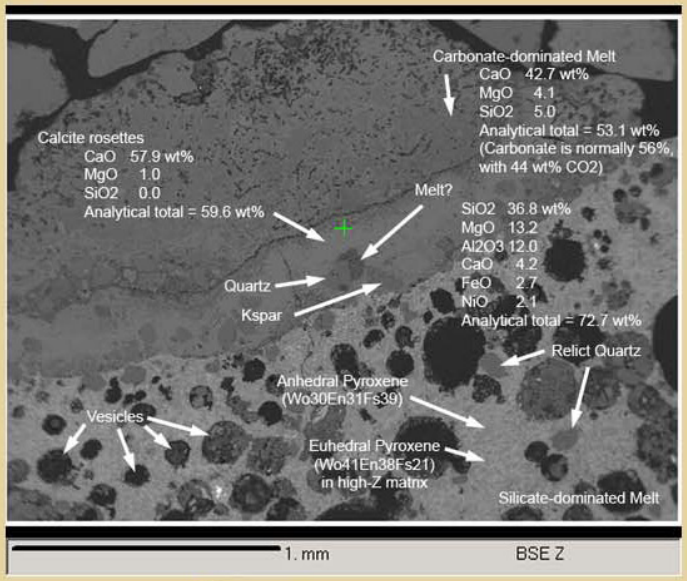

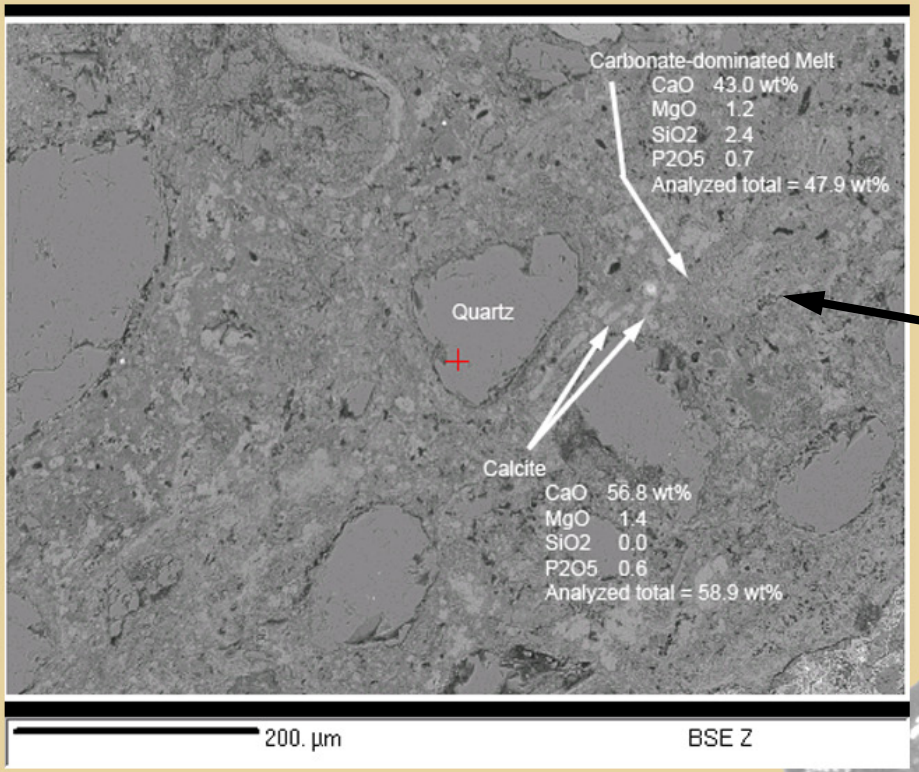


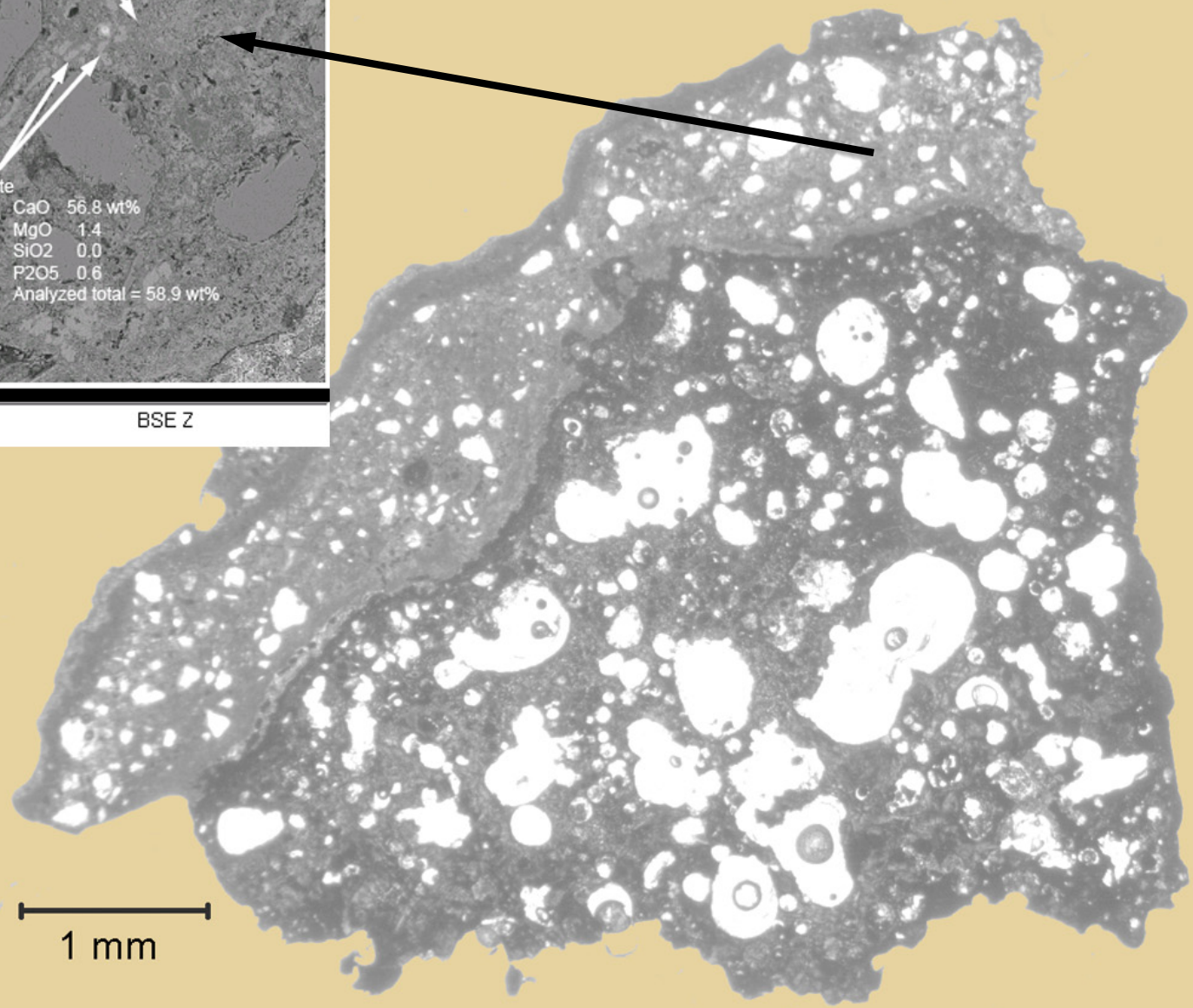


Fig. 4.3. Compound impact melt particle, shown in thin-section (right). The bulk of this melt particle is composed of a highly vesicular mafic silicate melt. This melt is similar to those described by Horz *et al*. (2002), which formed from impact melted and thoroughly degassed Kaibab dolomite, with variable contributions from the projectile (mostly Fe and Ni), Moenkopi siltstone (Si), and Coconino sandstone (Si). This silicate-dominated melt is coated with carbonate-dominated melt with entrained relict quartz and tiny remnant carbonate, as shown in a close-up view using back-scattered electron imaging techniques (above). Interestingly, the carbonate grains are calcite, not dolomite. The silicate-dominated melt was apparently super-heated and completely degassed its $CO_2$, while the carbonate-dominated melt was quenched before $CO_2$ could be lost.